GROWTH OF INTERMEDIATE-MASS BLACK HOLES IN THE HIERARCHICAL FORMATION OF SMALL SPIRAL GALAXIES IN THE HIGH-z UNIVERSE

Nozomu Kawakatu

International School for Advanced Studies (SISSA/ISAS), Via Beirut 2-4, 34014 Trieste, Italy; kawakatu@sissa.it

Takayuki R. Saitoh

National Astronomical Observatory of Japan, Mitaka, Tokyo 181-8588, Japan; saitoh.takayuki@nao.ac.jp

AND

Keiichi Wada[1]

National Astronomical Observatory of Japan, Mitaka, Tokyo 181-8588, Japan; wada.keiichi@nao.ac.jp

ABSTRACT

Combining a theoretical model of mass accretion onto a galactic center with a high-resolution N-body/smoothed particle hydrodynamics (SPH) simulation, we investigate the formation of an intermediate-mass black hole (IMBH) during the hierarchical formation of a small spiral galaxy (with a total mass of $10^{10} \, M_{\odot}$) in the high-z universe. We found that the rate of average mass accretion to the nucleus due to the radiation drag exerted by newly formed stars in the forming galaxy is $\approx 10^{-5} \, M_{\odot} \, \mathrm{yr}^{-1}$. As a result of this accretion, an IMBH with $\approx 10^4 \, M_{\odot}$ can be formed in the center of the spiral galaxy at $z \sim 4$. We found that a central BH coevolves with the dark matter halo from $z \sim 15$ to 2. The mass ratio of the BH to the dark matter halo is nearly constant, $\approx (1$–$3) \times 10^{-6}$ from $z \sim 10$ to 2. This is because change in the dark matter potential enhances star formation in the central part of the galaxy, and as a result the BH evolves due to mass accretion via the radiation drag. Therefore, our model naturally predicts a correlation between massive BHs and dark matter halos. Moreover, it is found that the final BH-to-bulge mass ratio ($\approx 5 \times 10^{-5}$) in a small spiral galaxy at high-z is much smaller than that in the large galaxies ($\approx 10^{-3}$). Our results also suggest that the scatter in the observed scaling relations between the bulge mass and black hole mass are caused by a time lag between BH growth and growth of the bulge mass. We also predict that the X-ray luminosity of active galactic nuclei (AGNs) is positively correlated with the CO luminosity in the central region. By comparing our results with the properties of Lyman break galaxies (LBGs), it is predicted that some LBGs have massive BHs of $\approx 10^6$–$10^7 \, M_{\odot}$.

Subject headings: black hole physics — galaxies: nuclei — galaxies: starburst — hydrodynamics — methods: numerical — radiation mechanisms: general

1. INTRODUCTION

Recent compilation of the kinematical data on galactic centers has revealed that a central massive dark object (MDO), which is a candidate for a supermassive black hole (BH), tightly correlates with the mass of a galactic bulge; the BH-to-bulge mass ratio is ≈ 0.001 as a median value (e.g., Kormendy & Richstone 1995; Magorrian et al. 1998; Merritt & Ferrarese 2001; McLure & Dunlop 2002; Marconi & Hunt 2003). There have been a number of theoretical efforts to clarify the origin of this relation (e.g., Silk & Rees 1998; Ostriker 2000; Adams et al. 2001). However, little has been elucidated regarding the physics on the angular momentum transfer in a spheroidal system (a bulge), which is inevitable for formation of BHs. Recently, Ferrarese (2002) and Baes et al. (2003) have argued that the BH mass in spiral galaxies is related to the dark matter halo mass. This correlation suggests that formation of supermassive BHs is physically connected not only with formation of galactic bulges, but also with assembly processes of dark matter halos in galaxy formation. Since merging of protogalaxies triggers active star formation, a physical link between star formation and mass accretion toward the central BH is expected.

Umemura (2001) has considered the effects of radiation drag as a mechanism for removing the angular momentum of the gas in the active galactic nuclei. The radiation drag in the solar system is known as the Poynting-Robertson effect. Note that, in the early universe, Compton drag force has a similar effect on the formation of massive BHs (Umemura et al. 1993). The rate of angular momentum loss due to radiation drag is given by $d \ln J/dt \simeq -\chi_d E/c$, where J is the total angular momentum of the gaseous component, E is the energy density of the uniform spheroidal system, and χ_d is the mass extinction coefficient, which is given by $\chi_d = n_d \sigma_d / \rho_{\mathrm{gas}}$ with the number density n_d, cross section σ_d, and gas density ρ_{gas}. The exact expressions for the radiation drag are given in the literature (e.g., Umemura et al. 1997; Fukue et al. 1997).

In an optically thin regime, $d \ln J/dt \simeq -(\tau L_*/c^2 M_{\mathrm{gas}})$, where τ is the total optical depth of the system, L_* is the total luminosity of the spheroidal system, and M_{gas} is the total mass of gas. In an optically thick regime, the radiation drag efficiency is saturated due to conservation of the photon number (Tsuribe & Umemura 1997). Thus, an expression of the angular momentum loss rate suitable for both regimes can be $d \ln J/dt \simeq -(L_*/c^2 M_g)(1 - e^{-\tau})$. The mass accretion rate is therefore $\dot{M} = -M_g \, d \ln J/dt = (L_*/c^2)(1 - e^{-\tau})$. In an optically thick regime, this gives simply $\dot{M} = L_*/c^2$ (Umemura 2001). Thus, the total mass accreted onto the MDO, M_{MDO}, is maximally $M_{\mathrm{MDO}} \simeq \int L_*/c^2 \, dt$. For more realistic cases, we should take into account the inhomogeneity of the interstellar matter (ISM). In active star-forming galaxies, the ISM is observed to be highly inhomogeneous (Sanders et al. 1988; Gordon et al. 1997). In addition, high-resolution three-dimensional

hydrodynamic simulations have shown that multiple supernovae (SNe) in a galactic center form a quasi-stable inhomogeneous torus around a supermassive black hole (Wada & Norman 2002). In such inhomogeneous ISM, optically thin surface layers of optically thick clumpy clouds lose their angular momentum due to radiation drag, and eventually they accrete toward the galactic center (Sato et al. 2004). Kawakatu & Umemura (2002) have shown that the inhomogeneity of ISM plays an important role in the radiation drag attaining maximal efficiency. Based on the radiation drag model, Kawakatu et al. (2003) predict that a mass ratio between the black hole mass and the bulge mass, $M_{BH}/M_{bulge} \simeq 0.001$, which is determined by the energy conversion efficiency of nuclear fusion from hydrogen to helium, i.e., 0.007 (Umemura 2001). In these previous studies, galaxies are treated as a one-zone model; therefore, the growth of supermassive BHs has not been revealed in a more realistic situation, namely that of the hierarchical formation of galaxies. Granato et al. (2004) presented a semianalytic modeling of the early evolution of massive spheroidal galaxies and active galactic nuclei (AGNs) within the dark matter halo, including the angular momentum transfer via radiation drag. They claimed that the feedback from supernovae and from AGNs determines the relation between the BH mass, the bulge mass, and the dark matter halo mass (see also Bukert & Silk 2001).

Di Matteo et al. (2003) followed the evolution of the gas, stars, and the dark matter in forming galaxies, and they found that the observed BH mass-to-stellar velocity dispersion of a bulge is reproduced if the gas mass in the bulge is linearly proportional to the black hole mass. However, it is impossible to resolve the structure of the central subkiloparsec region or the bulge component of host galaxies because of the limitation on their numerical resolution (mass resolutions are 10^7–10^8 $M_\odot$, and gravitational softening lengths are 4–9 kpc). Recently, using high-resolution cosmological N-body/smoothed particle hydrodynamics (SPH) simulations with 2×10^6 particles (one SPH particle has 10^3 $M_\odot$ and a gravitational softening length of ~50 pc), Saitoh & Wada (2004) investigated stellar and gaseous cores on a subkiloparsec scale during the hierarchical formation of a small spiral galaxy (with a total mass of 10^{10} $M_\odot$) and found that the galactic core (<several 100 pc) coevolves with the galactic dark matter halo of ~10 kpc scale. The rapid increase of the gas mass and star formation rate (SFR) in the central subkiloparsec region may cause further mass accretion to the nucleus due to, for example, a turbulent viscosity (Wada et al. 2002), a gas drag and dynamical friction in dense stellar clusters (Norman & Scoville 1988), the radiation drag originating in the nuclear starburst (e.g., Umemura 2001), or the BHs-BHs merger (e.g., Haehnelt 2004).

Here we focus on the radiation drag as one of the possible processes of mass accretion onto a BH during hierarchical formation of a galaxy. The observed AGN-starburst connection in nearby galaxies (Heckman et al. 1989; Kauffman et al. 2003; Imanishi & Wada 2004; Jahnke et al. 2004) suggests that star formation plays an important role in the mass accretion. We expect a correlation between BHs and bulges as a natural result of galaxy formation, if the radiation drag works. In this paper, we quantitatively estimate the evolution of a black hole mass in a forming galaxy, combining N-body/SPH simulations of cosmological galaxy formation done by Saitoh & Wada (2004) with an analytic model of angular momentum transfer due to the radiation drag.

This paper is organized as follows. In § 2 we briefly describe the simulation of galaxy formation. Our model for the growth of a massive BH via the radiation-hydrodynamic process is also explained. Based on this model, in § 3 we show the history of accretion to a BH in a spiral galaxy. We also discuss the mutual

relationships between a massive BH, a galactic bulge, and a dark matter halo. Finally, we discuss correlation between AGN activities and the properties of bulges. In § 4 we compare our predictions with observational scaling relations, and we discuss the Lyman break galaxies (LGBs), as candidates for the small spiral galaxies that we demonstrate here. Section 5 is devoted to conclusions.

2. MODELS

2.1. *Simulations of Galaxy Formation*

The numerical simulations used here are based on Saitoh & Wada (2004) and R. Saitoh et al. (2005, in preparation). We model the formation and evolution of galaxies in the cold dark matter (CDM) universe, adopting a top-hat initial condition with an open boundary for a single galactic halo ($M_{halo} \sim 10^{10}$ $M_\odot$). The cosmological parameters in our model are $\Omega_0 = 1.0$, $\Omega_\lambda = 0.0$, $\Omega_b = 0.1$, $h = H_0$ km^{-1} s^{-1} Mpc^{-1} = 0.5, and $\sigma_8 = 0.63$. The collapse epoch of the halo is set at $z_c \sim 3$, and its spin parameter is 0.05 (Barnes & Efstathiou 1987; Heavens & Peacock 1988).

Since the total mass of the object in our simulation is small (10^{10} $M_\odot$), evolution of the system, and therefore the conclusion in this paper, do not depend on the employed cosmology. The collapse epoch of the object in our simulation is $z_c \sim 3$, for which the evolution is not strongly affected by the Λ term. This is in contrast to much larger systems, such as clusters of galaxies.

The number of baryon (SPH) and dark matter particles in the spherical region is $N_{SPH} = N_{DM} = 1,005,600$. The mass resolutions of baryon (gas and stars converted from the gas) and DM particles are 1.1×10^3 and 1.0×10^4 $M_\odot$, respectively. The gravitational softening lengths are 52 pc for baryon particles and 108 pc for DM particles. The initial distribution of the particles is generated by COSMICS (Bertschinger 2001). We discuss the evolution of galaxies until $z = 2$, because the assembly history for the boundary conditions would not be realistic much later than the collapse epoch, z_c. However, $z \sim z_c$ the assembly of the simulated galaxy finishes, so that the mass of the galaxy at $z = 0$ would be equal to that at $z = 2$.

The numerical technique we employ to represent the evolution of galaxies is a standard hybrid N-body/hydrodynamic code for galaxy formation. The code includes both the radiative cooling and star formation. However, the dynamical and radiative feedback processes from star formation and supernova explosions are not explicitly taken into account. The length of the interaction list of each SPH particle is $N_{NB} = 50$. In the SPH simulations, the Jeans instability can be resolved correctly for masses larger than $2N_{NB}m_{SPH}$ (Bate & Burkert 1997), where m_{SPH} is mass of an SPH particle. In the simulation, we can resolve the gravitational instability of a cloud whose mass is larger than 1.1×10^5 $M_\odot$. In order to model the multiphase nature of the interstellar medium (e.g., Wada & Norman 2001), we solve the energy equation with the radiative cooling under 10^4 K and the inverse Compton cooling. We assume that the gas has a primordial abundance of $X = 0.76$ and $Y = 0.24$, and we assume an ideal gas with $\gamma = 5/3$. The mean molecular weight of gas, μ, is set to 0.59.

The star formation algorithm is similar to the one by Katz (1992). If an SPH particle satisfies all the following conditions: (1) the regions are in virialized halos ($\rho_{SPH} > 200\rho_{BG}$), where ρ_{BG} is the background density; (2) low temperature ($T < 3 \times 10^4$ K); and (3) collapsing regions ($\nabla \cdot \boldsymbol{u} < 0$), then it is converted into a collisionless star particle inheriting the velocity and the mass of the gas particle. The local SFR is assumed to be SFR = $c_* m_{SPH}/\tau_{ff}$, with $c_* = 1/30$ (e.g., Abadi et al. 2003), where $\tau_{ff} = 1/(G\rho_{SPH})^{1/2}$ is a free-fall time.

2.2. *Radiation Drag Model*

Next, we model the BH growth, based on the radiation drag–driven mass accretion. Here, we suppose a two-component system: an inhomogeneous ISM with disklike geometry embedded in a spheroidal stellar bulge. In fact, the ISM in active star-forming galaxies is highly inhomogeneous (Sanders et al. 1988; Gordon et al. 1997). Wada & Norman (2002) also showed that the multiple SNe in a galactic center from a quasi-stable inhomogeneous torus around a supermassive BH.

We assume that stars and $N_c(=10^4)$ identical clouds are randomly distributed in a system of the bulge.[2] The optical depth of a gas cloud is $\bar{\tau} = \chi_d \rho_{\mathrm{gas}} r_c \simeq \chi_d m_{\mathrm{gas}}/r_c^2$, where ρ_{gas}, m_{gas}, and r_{gas} are the density, mass, and size of a cloud. The mass extinction coefficient χ_d is given by $\chi_d = n_d \sigma_d / \rho_{\mathrm{gas}}$ with the number density n_d, cross section σ_d, and gas density ρ_{gas}. In this paper, we assume $\chi_d = 300$ cm^2 g$^{-1}(a_d/0.1 \ \mu\mathrm{m})^{-1}(\rho_s/\mathrm{g \ cm^{-3}})(Z/0.3 \ Z_\odot)$, where a_d is the grain radius, ρ_s is the density of solid material density within the grain (e.g., Spitzer 1978; their § 9.3), and Z is the metallicity of gas, which are fixed at $a_d = 0.1 \ \mu$m, $\rho_s = 1$ g cm^{-3}, and $Z = 0.3 \ Z_\odot$.[3] The total optical depth of the bulge, τ_{bulge}, is given by $\tau_{\mathrm{bulge}} = \bar{\tau} \bar{N}_{\mathrm{int}}$, where $\bar{N}_{\mathrm{int}}$ is the average number of clouds intersected by a light ray over a bulge scale. The $\bar{N}_{\mathrm{int}}$ is defined by $\bar{N}_{\mathrm{int}} = n_c \pi r_c^2 r_{\mathrm{bulge}} = (3/4)N_c(r_c/r_{\mathrm{bulge}})^2$, where $n_c = N_c/(4/3)\pi r_{\mathrm{bulge}}^3$ is the number density of gas clouds. In this paper, we assume that the cloud covering factor is of order unity, i.e., $\bar{N}_{\mathrm{int}} \approx O(1)$, according to the previous analysis. A different level of ISM clumpiness can reduce the radiation drag efficiency by a factor of 2 (Kawakatu & Umemura 2002). We also confirm that the optical depth in a clumpy media is an order of unity, using a three-dimensional hydrodynamic simulation (see Fig. 1 in Wada & Norman 2002). Even if the system is extremely gas rich ($M_{\mathrm{gas}} = 10^8 \ M_\odot$ in the central 100 pc), we find that the optical depth for the disk plane from various directions is distributed between 0.5 and 1.2, assuming the same gas/dust ratio and dust opacity in the analysis here. Finally, using $M_{\mathrm{gas}} = N_c m_{\mathrm{gas}}$, the total optical depth of the bulge can be rewritten as

$$\tau_{\mathrm{bulge}}(t) = \bar{\tau}(t) \bar{N}_{\mathrm{int}} \simeq \frac{3\chi_d}{4\pi} \frac{M_{\mathrm{gas}}(t)}{r_{\mathrm{bulge}}^2(t)}, \qquad (1)$$

where $r_{\mathrm{bulge}}(t)$ and $M_{\mathrm{gas}}(t)$ are the size and the gas mass of the bulge.[4]

The radiation drag, which drives the mass accretion, originates in the relativistic effect in absorption and subsequent reemission of the radiation. This effect is naturally involved in relativistic radiation hydrodynamic equations (Umemura et al. 1997; Fukue et al. 1997). The angular momentum transfer in radiation hydrodynamics is given by the azimuthal equation of motion in cylindrical coordinates,

$$\frac{1}{r} \frac{d(rv_\phi)}{dt} = \frac{\chi_d}{c} \left[F^\phi - (E + P^{\phi\phi})v_\phi \right], \qquad (2)$$

where E is the radiation energy density, F^ϕ is the radiation flux, and $P^{\phi\phi}$ is the radiation stress tensor. By solving radiative transfer including dust opacity, we evaluate the radiative quantities, E, F^ϕ, and $P^{\phi\phi}$, and thereby obtain the total angular momentum loss rate. Then, we can estimate the mass accretion rate of the dusty ISM accreted onto a central massive dark object, $\dot{M}_{\mathrm{MDO}}$, by using the relation $\dot{M}_{\mathrm{drag}}/M_{\mathrm{gas}} = -\dot{J}/J$, where J and M_{gas} are the total angular momentum and gas of ISM. In the optically thick regime of the radiation drag, $-M_{\mathrm{gas}}\dot{J}/J = L_{\mathrm{bulge}}(t)/c^2$, where $L_{\mathrm{bulge}}(t)$ is the total luminosity of the bulge. The radiation drag efficiency depends on the optical depth τ_{bulge} in proportion to $(1 - e^{-\tau_{\mathrm{bulge}}(t)})$ (Umemura 2001). Thus, the mass accretion rate via the radiation drag is

$$\dot{M}_{\mathrm{drag}} = \eta_{\mathrm{drag}} \frac{L_{\mathrm{bulge}}(t)}{c^2} \left(1 - e^{-\tau_{\mathrm{bulge}}(t)} \right), \qquad (3)$$

where $L_{\mathrm{bulge}}(t)$ and $\tau_{\mathrm{bulge}}(t)$ are the total luminosity and the time-dependent total optical depth of the bulge. Kawakatu & Umemura (2002) found that the efficiency η_{drag} is maximally 0.34 in the optically thick regime.

The radiation energy emitted by a main-sequence star is 0.14ϵ to the rest-mass energy of the star, where ϵ is the energy conversion efficiency of the nuclear fusion from hydrogen to helium, which is 0.007. Thus, the luminosity of the bulge at optical and UV bands is simply approximated by $L_{\mathrm{bulge}}(t) \simeq 0.14\epsilon\dot{M}_{\mathrm{bulge}}(t)c^2$, where $\dot{M}_{\mathrm{bulge}}(t)$ is the SFR in the bulge. Here, we employ a stellar initial mass function (IMF) such that $\phi = dn/d\log m_* = A(m_*/M_\odot)^{-\alpha}$ for a mass range of (m_l, m_u), where m_*, m_l, and m_u are the stellar mass, the lower mass, and the upper mass, respectively. We assume that $m_l = 0.1$ and $m_u = 60 \ M_\odot$, and the index α is 1.35.[5] The accretion rate (eq. [3]) is therefore

$$\dot{M}_{\mathrm{drag}} \simeq 1.2 \times 10^{-3}\eta_{\mathrm{drag}}\dot{M}_{\mathrm{bulge}}(t)(1 - e^{-\tau_{\mathrm{bulge}}(t)}). \qquad (4)$$

Here we ignore the infrared luminosity from the evolved stars because the dust opacity for the infrared band is much smaller than that for the optical and UV bands; $\dot{M}_{\mathrm{bulge}}$ and $\tau(t)$ are directly given from the numerical simulations. The total mass of dusty ISM accreted to the central massive dark object (MDO), $M_{\mathrm{MDO}}(t)$, is obtained by

$$M_{\mathrm{MDO}}(t) = \int_0^t \dot{M}_{\mathrm{drag}} \, dt. \qquad (5)$$

As seen in equations (3), (4), and (5), the linear relation between the MDO mass and the bulge mass is a direct result of the radiation drag mechanism. The possible mass accreted by the radiation drag in the optically thick limit is given by

$$M_{\mathrm{MDO,max}} = \eta_{\mathrm{drag}} \int_{t_0}^{t_1} L_{\mathrm{bulge}}/c^2 \, dt \simeq 5 \times 10^{-3} M_{\mathrm{bulge}}, \quad (6)$$

where t_0 is 0.1 Gyr ($z \sim 25$), which corresponds to the epoch where we first detect the progenitor of galaxy, and t_0 is 2.6 Gyr ($z \sim 2$). The correspondence between time and redshift is based on the cosmological model we adopted.

In this model, we should distinguish the BH mass from that of an MDO, although the mass of an MDO is often regarded as BH mass from an observational point of view. The radiation drag is

---

[2] It is noted that simulations with a 3 times larger number of clouds did not lead to any fundamental difference for final BH mass, although at least 10^4 clouds are necessary to treat the radiation transfer effect properly in clumpy ISM. The total optical depth, τ_{bulge}, is not also significantly affected by changing the cloud size, r_c.

[3] We should keep in mind that recent observations suggest that the metallicity of the gas in the AGNs can be supersolar $Z > Z_\odot$ (e.g., Ohta et al. 1996; Dietrich & Wilhelm-Erkens 2000; Maiolino et al. 2003). If this is the case, then the optical depth of a gas cloud can be enhanced by a factor of 3–4.

[4] In the present paper, we identify a "bulge" as a spheroidal star-forming region where the average number density of the gas, n_H, is larger than 0.1 cm^{-3} in a spiral galaxy. This criterion corresponds to the density criterion of the star-forming region.

[5] As for the effect of IMF, if the slope and the mass range of IMF are changed to satisfy the spectrophotometric properties of galactic bulges, then the radiation drag efficiency is altered by a factor of ±50% (Kawakatu & Umemura 2004).
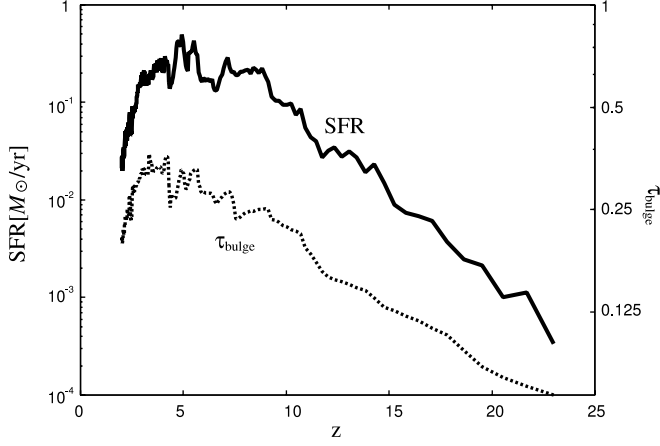
Fig. 1.—Redshift evolution of the star formation rate (in units of $M_\odot$ yr^{-1}) and total optical depth ($\tau_{\rm bulge}$) of the bulge at redshift (z). At $z > 4$, both the SFR and the optical depth increase with time, while they decrease at low-z ($z < 4$).

not likely to remove the angular momentum thoroughly, and thus some residual angular momentum will terminate the radial contraction of the accreted gas (Sato et al. 2004). Hence, the dusty ISM probably forms a compact rotating torus. In this nuclear torus, we suppose that the mass accretion onto the BH horizon is determined by the Eddington rate and that the BH mass grows according to

$$M_{\rm BH}(t) = M_0 e^{t/t_{\rm Edd}}, \qquad (7)$$

where $t_{\rm Edd}$ is the Eddington timescale, $t_{\rm Edd} = \eta_{\rm BH} M_{\rm BH} c^2 / L_{\rm Edd}$, with the energy conversion efficiency, $\eta_{\rm BH}$, and the Eddington luminosity, $L_{\rm Edd}$. Unless otherwise stated, $\eta_{\rm BH}$ is assumed to be 0.42, which is the conversion efficiency of an extreme Kerr BH. Recently, Shibata (2004) has found that a rigidly rotating very massive star (VMS) with several 100 $M_\odot$ can be unstable for a softer equation of state, and eventually it forms a BH. In addition, the theory of stellar evolution reveals that the nuclear burning in VMSs above 260 $M_\odot$ is unable to halt gravitational collapse (e.g., Heger et al. 2003). Thus, the VMSs inevitably evolve into massive BHs without supernova explosions. Here, we assume 260 $M_\odot$ as the mass of the seed black hole M_0.

3. RESULTS

On the basis of the coevolution model described in the previous section, we estimate the mass accretion driven by the radiation drag during hierarchical galaxy formation. Next, we reveal the relationship between the growth of a BH and that of a dark matter halo. Finally, we discuss the relation between AGN activity and the properties of the bulges.

3.1. Mass Accretion Rate via Radiation Drag

Evolution of the SFR and the optical depth of bulge ($\sim$1 kpc) are shown in Figure 1. Before $z \sim 4$, the SFR and the optical depth increase, while they decrease rapidly for $z < 4$. This can be understood as follows. At high-z ($z > 4$), the supply of the gas due to mergers of smaller protogalaxies and consumption of the gas in the central part of the galaxy (bulge) are almost balanced. Thus, both the SFR and the optical depth are enhanced. At low-z ($z < 4$), accretion of the gas to the bulge associated with merger events is decreased. The gas in the bulge is consumed by the star formation. As a result, it makes the gas of the bulge poor. As seen in Figure 1, we found that the evolution of the SFR and the
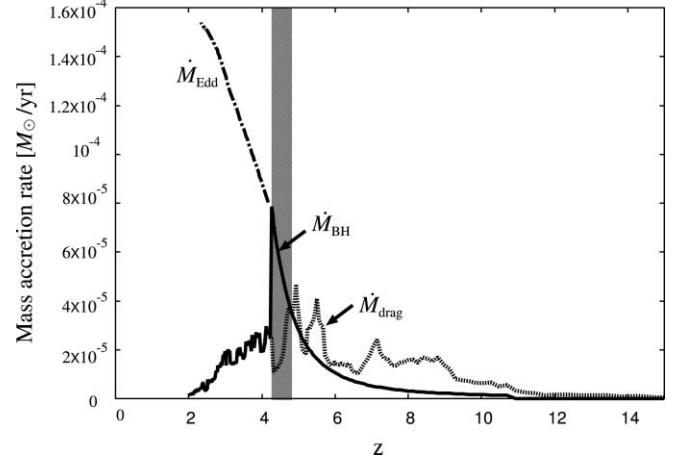
Fig. 2.—Same as Fig. 1, but for the mass accretion rate due to the radiation drag ($\dot{M}_{\rm drag}$), the mass accretion rate onto a BH ($\dot{M}_{\rm BH}$), and the Eddington mass accretion rate ($\dot{M}_{\rm Edd}$). The averaged mass accretion rate due to the radiation drag is a few 10^{-5} $M_\odot$ yr^{-1}, which is comparable to the Eddington mass accretion rate for a black hole mass with $\approx 10^4$ $M_\odot$. After $z \simeq 5$, $\dot{M}_{\rm Edd}$ exceeds $\dot{M}_{\rm drag}$. For $z < 4$, $\dot{M}_{\rm BH}$ follows $\dot{M}_{\rm drag}$, because the mass of the BH reaches that of MDO at $z \approx 4$ (see also Fig. 3). The shaded area ($4.2 < z < 4.8$) corresponds to the BH growing phase ($\dot{M}_{\rm BH} > \dot{M}_{\rm drag}$).

optical depth are not smooth, but episodic. This episodic growth corresponds to the phase of the high mass accretion onto the bulge component triggered by major mergers with some time delays, which are typically 10^7 yr (for details, see Saitoh & Wada 2004).

Figure 2 shows the evolution of the mass accretion rate due to the radiation drag ($\dot{M}_{\rm drag}$), the rate of mass accretion onto a BH ($\dot{M}_{\rm BH}$), and the Eddington mass accretion rate ($\dot{M}_{\rm Edd}$). It is clear that $\dot{M}_{\rm drag}$ is also episodic, reflecting the evolution of the SFR and optical depth (Fig. 1 and eq. [4]). We have also found that the averaged mass accretion rate is $\approx 10^{-5}$ $M_\odot$ yr^{-1}. This rate is comparable to the Eddington mass accretion rate for a black hole mass with 10^4 $M_\odot$, that is,

$$\dot{M}_{\rm Edd} = \frac{1}{\eta_{\rm BH}} \frac{L_{\rm Edd}}{c^2} \approx 10^{-5} \ M_\odot \ {\rm yr}^{-1} \left(\frac{\eta_{\rm BH}}{0.42} \right)^{-1} \left(\frac{M_{\rm BH}}{10^4 \ M_\odot} \right). \quad (8)$$

In Figure 2, the Eddington mass accretion rate (eq. [8]) is larger than $\dot{M}_{\rm drag}$ after $z \sim 5$. Since the BH mass equals the mass of MDO at $z \approx 4$ (see Fig. 3), the mass accretion onto the BHs after $z \sim 4$ would be controlled by the mass accretion to the MDO via the radiation drag, i.e., $\dot{M}_{\rm BH} = \dot{M}_{\rm drag}$. Figure 2 shows that $\dot{M}_{\rm BH} > \dot{M}_{\rm drag}$ in a period of $4.2 < z < 4.8$ (Fig. 2, *shaded area*). In this paper, we call this period a "BH-growing phase," which is $\approx 10^8$ yr.

3.2. Coevolution of MBHs, Bulges, and Dark Matter Halos

Figure 3 shows the evolution of masses of the dark matter ($M_{\rm halo}$), the stellar component in the bulge ($M_{\rm bulge}$), the gas in the bulge ($M_{\rm gas}$), MDO ($M_{\rm MDO}$), and the massive BH ($M_{\rm BH}$); $M_{\rm halo}$, $M_{\rm bulge}$, and $M_{\rm gas}$ are directly obtained from the numerical simulation of galaxy formation (§ 2.1), and we obtain $M_{\rm MDO}$ and $M_{\rm BH}$ from $\dot{M}_{\rm drag}$ and $\dot{M}_{\rm BH}$ (Fig. 2).

The BH mass reaches $M_{\rm MDO}$ at $z \approx 4$. As seen in Figure 3, during $z > 4$, the massive black hole (MBH) grows due to the Eddington mass accretion. At $z < 4$, the growth rate of the MDO is reduced because $\dot{M}_{\rm drag}$ becomes smaller than $\dot{M}_{\rm Edd}$, and $\dot{M}_{\rm drag}$ declines owing to the decrease in the SFR and the optical depth of bulges (Fig. 1). As a result, we find that an intermediate MBH
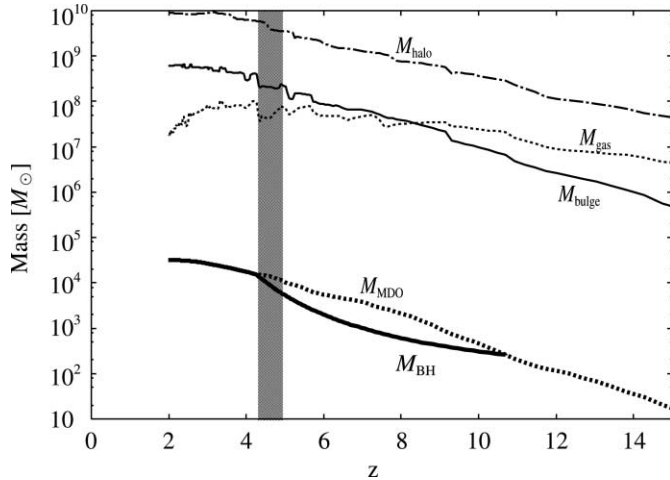
FIG. 3.—Same as Fig. 1, but for masses of the dark halo (M_{halo}), gas (M_{gas}), and bulge (M_{bulge}). Evolution of the mass of black hole (BH) and the massive dark object (MDO) are also plotted. The mass of the seed black hole is assumed to be $M_0 = 260\ M_\odot$ (see eq. [7]), M_{bulge} and M_{gas}, respectively, while M_{MDO} is the mass of MDO and M_{BH} is the mass of the massive BH. It shows that the MDO mass is proportional to the bulge mass. The BH mass reaches the MDO mass at $z \approx 4$.

(IMBH) with $\approx 3 \times 10^4\ M_\odot$ can be formed at $z \sim 2$ in a small spiral galaxy (with a total mass of $10^{10}\ M_\odot$). At $z = 2$, the growth of the simulated galaxy finishes, so that the BH growth also would stop after $z = 2$ because of the lack of gas in the bulge. In Figure 3, it is also found that the significantly massive dusty torus with $M_{MDO} > M_{BH}$ exists in the early phase of the BH growth ($z \approx 5$). The massive torus, itself produced by the starburst in bulges, would obscure the nucleus in the edge-on view and make a type 2 nucleus. Therefore, it is suggested that not only a nuclear starburst in a torus around a supermassive BH like an MDO (Ohsuga & Umemura 1999; Wada & Norman 2002; Watabe & Umemura 2005), but also a starburst in a bulge may contribute to the AGN obscuration in the BH growing objects.

Figure 4 shows the evolution of mass ratios between the BH and the bulge or the halo, i.e., M_{BH}/M_{bulge} and M_{BH}/M_{halo}. We find that before $z \approx 8$, the growth of the bulge and dark matter halo are faster than that of the BH. After $z \approx 8$, the mass ratios
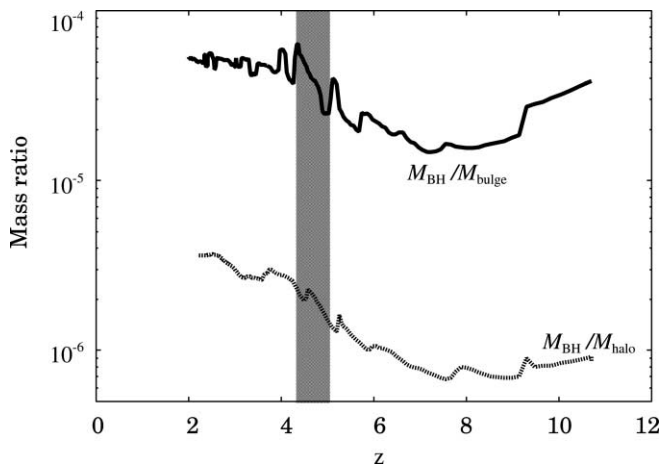
FIG. 4.—Evolution of the mass ratios, M_{BH}/M_{bulge} and M_{BH}/M_{halo}, against the redshift. The mass ratios are nearly constant within a factor of 2–3, but before $z > 8$, growth of the BH is slower than that of the bulge. Note that the mass ratios increase more rapidly during the BH growing phase (the shaded area, which lasts $\approx 10^8$ yr). After $z \sim 4$, the mass ratios are almost constant, with $M_{BH}/M_{bulge} \approx 5 \times 10^{-5}$ and $M_{BH}/M_{halo} \approx 3 \times 10^{-6}$.
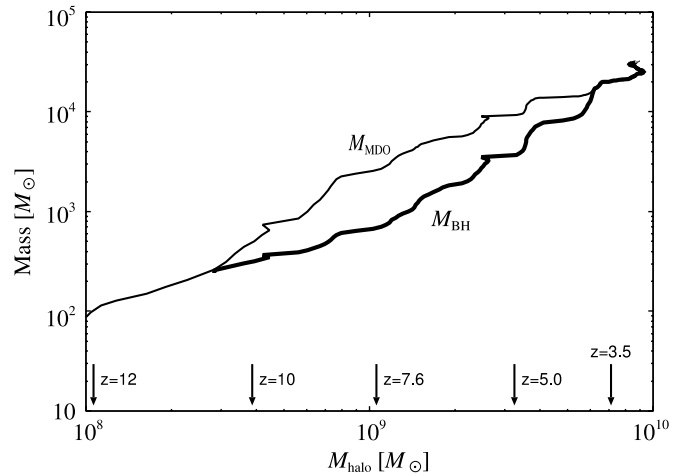
FIG. 5.—Masses of the BH (*thick line*) and MDO (*thin line*) are plotted against the mass of the dark halo. The arrows indicate the masses of the dark halo at labeled redshifts. It shows that the BH coevolves with the dark matter halo from $z \sim 10$ to 2.

increase with time because the growth of the BH is dominated by the Eddington mass accretion rate, and the rate is increasing exponentially (see Fig. 2). One should note, however, that the mass ratios change by a factor of 2–3 in the BH-growing phase ($\approx 10^8$ yr). This change is caused by a time lag between the BH growth and the growth of the bulge or the halo. If this is also the case in real galaxies, then the scatter in the observed M_{BH}-M_{bulge} relation may be because of this time lag. On the other hand, the mass of the MDO equals that of the BH ($z < 4$), and the mass ratios do not significantly change with $M_{BH}/M_{bulge} \approx 5 \times 10^{-5}$ and $M_{BH}/M_{halo} \approx 3 \times 10^{-6}$. Therefore, we would predict that the scatter in the scaling relation is larger in the BH-growing objects at high-z than in nearby, well-evolved galaxies.

In Figure 5, we plot the mass of the MDO and the BH against the halo mass. This reveals that the MDO and the BH coevolve with the dark matter halo from $z \sim 10$ to 2. The masses of the MDO and the BH increase with the development of the dark halo. The mass ratio of the BH to the halo (M_{BH}/M_{DM}) increases gradually from 10^{-6} to 3×10^{-6} from $z \sim 7$ to 2 (see also Fig. 4).

From these arguments, the M_{BH}-M_{halo} correlation indicates that variation of the dark matter halo potential associated with merging processes positively links with the mass accretion toward the galactic center via the radiation drag. Our model suggests that a BH mass is mutually related to the mass of a bulge and that of a dark matter halo throughout the history of the galaxy formation. Comparison with observations is discussed in § 4.

3.3. AGN Activity–Host Relation

In this section, we examine the relation between the AGN activities and the properties of bulge components. Evolution of the bulge luminosity (L_{bulge}) at the optical and UV bands and the AGN luminosity (L_{AGN}) are plotted in Figure 6. During $z > 4$, the AGN luminosity increases with the time, because the mass accretion is determined by the Eddington rate. After $z \sim 4$, the AGN luminosity is limited by $\dot{M}_{drag}$ (see Fig. 3). Thus, the AGN luminosity exhibits a peak around $z \sim 4$, when $M_{MDO} \sim M_{BH}$. As seen in this figure, the AGN luminosity is always smaller than the bulge luminosity; in other words, no quasar phase, i.e., AGN luminosity–dominant phase, appears. However, the luminosity ratio of the AGN to the bulge exhibits the maximal value ($L_{AGN}/L_{bulge} \approx 0.1$) at $z \sim 4$. This suggests that some small
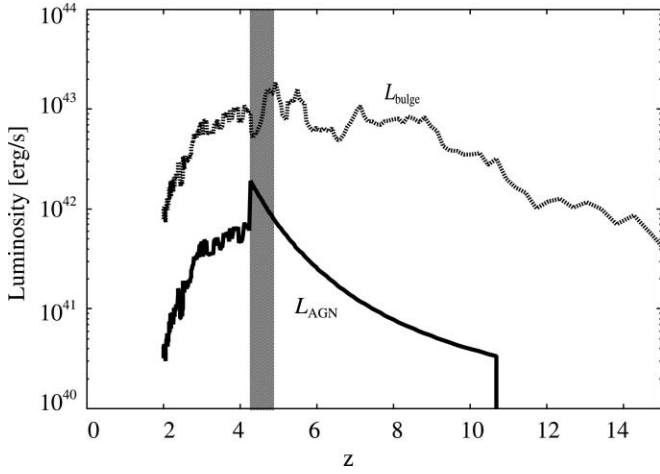
Fig. 6.—AGN and bulge luminosity as a function of redshift. Here, we assume that L_{AGN} is the Eddington luminosity before $z \sim 4$. After $z \sim 4$, the AGN luminosity is determined by the mass accretion due to the radiation drag. After the AGN luminosity exhibits a peak around $z \sim 4$, it fades out. At $z \approx 4$, the luminosity ratio of the AGN to the bulge exhibits the maximal value ($L_{AGN}/L_{bulge} \approx 0.1$).

Fig. 7.—Relation between the CO luminosity (L_{CO}) and the X-ray luminosity (L_X) during the evolution of the BH and the galaxy. The filled circles show time evolution in our model. The X-ray luminosity is positively correlated with the CO luminosity. The thin line represents this correlation, i.e., $\log L_X (\mathrm{ergs\ s^{-1}}) \sim 38 + 2 \log L_{CO} (\mathrm{K\ km\ s^{-1}\ kpc^2})$. The shaded area corresponds to the BH growing phase ($4.2 < z < 4.8$). The arrows show time evolution in the BH growing phase.

spiral galaxies at high-z could show the same level of typical low-luminosity AGNs in the local universe.

Figure 7 shows the relation between the X-ray luminosity, L_X, of the AGN and the CO luminosity, L_{CO}, of the bulge. Here, the X-ray luminosity L_X is estimated assuming $L_X = \epsilon_X L_{AGN}$, where ϵ_X is the X-ray–emitting efficiency, which is supposed to be 0.1. The CO luminosity is derived from the gaseous mass assuming a conversion factor, $X_{CO} = M_{gas}/L_{CO} = 4.6\ M_\odot/\mathrm{K\ km\ s^{-1}\ pc^2}$ (de Breuck et al. 2003). We found that the X-ray luminosity is positively linked with the CO luminosity for a wide range of luminosities, i.e., $L_X \sim 10^{38} (\mathrm{ergs\ s^{-1}})(L_{CO}/\mathrm{K\ km\ s^{-1}\ kpc^2})^2$.

In Figure 7, we also find that some points obviously deviate from the linear relation. These points correspond to the BH-growing phase ($4.2 < z < 4.8$; the shaded area in Figs. 2, 3, 4, and 6). This deviation implies that the growth of the BH via the Eddington mass accretion is much faster than that of gas mass in the bulge in this phase (see Fig. 3). In other words, except for the BH-growing phase, our result shows that the time-scale of the BH growth is comparable to that of the growth of the gas component in the bulge. Hence, by using the deviation from the linear relation for the L_X-L_{CO} diagram, we may look for the BH growing objects at high-z that we have missed so far.

4. COMPARISON WITH OBSERVATIONS

4.1. Massive BHs in Lyman Break Galaxies

In the present model, we have revealed that a small spiral galaxy (with a total mass of $10^{10}\ M_\odot$) can have an IMBH with $\approx 10^4$–$10^5\ M_\odot$ at $z \sim 2$. This is consistent with the mass range of the massive BH in dwarf galaxies with AGNs in the local universe (Barth et al. 2004, 2005; Greene & Ho 2004). Moreover, according to Figure 6, the AGN luminosity exhibits a peak around $z \approx 4$ (BH growing phase). This phase has several characteristic properties. (1) The X-ray luminosity of the AGN is relatively low, $L_X \approx 5 \times 10^7\ L_\odot$, if $L_X = 0.1 L_{AGN}$. (2) The luminosity of the bulge at the optical and UV bands is $5 \times 10^9\ L_\odot$. (3) The SFR is $\approx 0.3\ M_\odot\ \mathrm{yr^{-1}}$. (4) The stellar mass is $\approx 10^8\ M_\odot$. (5) An IMBH of $\approx 10^4\ M_\odot$ exists in the bulge. (6) The total optical depth of the bulge is $\tau_{bulge} \approx 0.4$.

As for the host galaxy, it has recently been suggested that LBGs, which are starburst galaxies at high-z, may be in the

forming phase of a galactic bulge (Friaca & Terlevich 1999; Matteucci & Pipino 2002). The SFR in the LBGs is ~ 3–$300\ M_\odot$ $\mathrm{yr^{-1}}$. LBGs have a typical luminosity $\sim 10^{10}$–$10^{11}\ L_\odot$, a stellar mass $\sim 10^{10}$–$10^{11}\ M_\odot$, and are observed to be optically thin (e.g., Shapley et al. 2001). They also exhibit strong clustering at $z \sim 3$, suggesting that hierarchical clustering is ongoing. In addition, the *Chandra X-Ray Observatory* has detected the hard X-ray of LBGs at $z = 2$–4 with the luminosity of $\sim 10^8\ L_\odot$, although it is still uncertain whether the X-ray emission arises from AGNs (Brandt et al. 2001). Comparing these properties of LBGs with our predictions (i.e., eqs. [1]–[6]), the small spiral galaxy (with a total mass of $10^{10}\ M_\odot$) in the BH-growing phase may correspond to low-mass counterparts of the LBGs. Extrapolating the scaling relation that we found to the observed LBGs, they would have the MBHs with $\approx 10^6$–$10^7\ M_\odot$. According to recent observations, only 3% of LBGs show AGN activity in the rest-frame hard X-ray band (Nandra et al. 2002) and optical band (Shapley et al. 2001). However, it has not been clear that this 3% fraction reflects the duty cycle of mass accretion to BHs (for details, see Shapley et al. 2001) or the possibility that the LBGs have massive BHs. Hosokawa (2004) claimed, assuming $M_{BH}/M_{bulge} \approx 0.001$, that $\sim 10\%$ of LBGs at $z \sim 3$ can have a massive BH with $\sim 10^7\ M_\odot$ to reproduce the local mass function of SMBHs (Salucci et al. 1999; Yu & Tremaine 2002; Aller & Richstone 2002; Shankar et al. 2004).

4.2. M_{BH}-M_{bulge} and M_{BH}-M_{halo} Relations

Barth et al. (2004) suggested that the correlation between BH mass and stellar velocity dispersion (the M_{BH}-σ relation) holds on a mass scale of an intermediate BH with $\approx 10^4$–$10^6\ M_\odot$. In addition, Baes et al. (2003) found a correlation between the BH mass and halo mass, i.e., $M_{BH}/10^8\ M_\odot \sim 0.11 (M_{halo}/10^{12}\ M_\odot)^{1.27}$, by using the M_{BH}-σ relation. This relation gives $M_{BH} = 3 \times 10^4\ M_\odot$ for $M_{halo} = 10^{10}\ M_\odot$, which is comparable to our prediction ($M_{BH} \approx 3 \times 10^4\ M_\odot$ at $z \sim 2$). However, it should be noted that there are large uncertainties in the empirical laws, as mentioned by Ferrarese (2002).

In our model, the final BH mass-to-bulge mass ratio is $\approx 5 \times 10^{-5}$, which is much smaller than the observed value ($\approx 10^{-3}$)

in nearby large galaxies. Thus, if our scenario is correct, it is expected that small spiral galaxies at high-z, which are not direct counterparts of the dwarf galaxies at low-z, could have the IMBHs and the smaller BH mass-to-bulge mass ratios. Currently, it is difficult to detect the IMBHs in small galaxies at high-z, and therefore we cannot directly prove our prediction, namely the small BH mass-to-bulge mass ratio. Moreover, there is also a room in the theoretical model, especially on the effects of mechanical, radiative, and chemical feedback processes from star formation. For instance, it is not trivial whether the stellar feedback affects on the SFR positively or negatively. Therefore, it is ultimately necessary to perform high-resolution radiative hydrodynamic simulations for galaxy formation taking into account these effects explicitly.

In this paper, we focus on the formation of a MBH due to the radiation drag in a small spiral galaxy. However, the process discussed here could be applied to more massive galaxies, because the transfer of the angular momentum via the radiation drag is independent of the mass scale of the galaxies. By using the BH mass-to-halo mass relation for a small spiral galaxy ($M_{\rm BH}/M_{\rm halo} \approx 10^{-6}$), we can predict that the massive spiral galaxies with $M_{\rm halo} = 10^{12}\ M_\odot$ have MBHs with 10^6–$10^7\ M_\odot$. In addition, the observations have suggested that the SFRs of the massive galaxies at high-z are 10–100 times higher than those of small galaxies like the one considered here. Thus, the final BHs might achieve $\approx 10^8\ M_\odot$, because the effect of the radiation drag is linearly proportional to the SFR (eq. [4]). If this is the case, then the host galaxies of the luminous quasars at high redshift would be starforming or post-starburst galaxies. On the other hand, we should note that the mass of a BH would depend on the morphology of the galaxies, even if the mass of the dark halo is the same. This is because the rate of mass accretion onto the BHs is not determined by the disk components, but by the bulge components in the host galaxies, due to the effects of geometric dilution and opacity (for details, see Kawakatu & Umemura 2004). Therefore, the morphology differences of host galaxies would cause the large scatter in the mass relation of the BHs to the halos in spiral galaxies. In fact, some authors claim that the $M_{\rm BH}$-$M_{\rm halo}$ relation is much weaker than the $M_{\rm BH}$-$M_{\rm bulge}$ relation in spiral galaxies (Salucci et al. 2000; Zasov et al. 2005).

4.3. $L_{\rm X}$-$L_{\rm CO}$ Relation

In § 3.3, we predicted that the X-ray luminosity of AGNs is positively correlated with the CO luminosity of bulges from $z \sim 10$ to 2. This correlation [i.e., $L_{\rm X} \sim 10^{38}({\rm ergs\ s^{-1}})(L_{\rm CO}/{\rm K\ km\ s^{-1}\ kpc^2})^2$], if we extrapolate it to AGNs with higher luminosity, is consistent with the $L_{\rm X}$-$L_{\rm CO}$ relation found in the low-redshift Seyfert galaxies and quasars (Yamada 1994). The observed $L_{\rm X}$-$L_{\rm CO}$ relation shows a scatter of about 1 order of magnitude. Suppose all galaxies follow the same $L_{\rm X}$-$L_{\rm CO}$ relation that we found here: we suspect that the large scatter in the ob-

served scaling relation was caused when the BHs were in their growing phases. Submillimeter observations by the Atacama Large Millimeter Array (ALMA) for luminous high-z quasars will be helpful for investigating the connection between the black hole mass and the host properties.

5. CONCLUSIONS

Combining a theoretical model of the mass accretion onto a galactic center due to the radiation drag with high-resolution N-body/SPH simulations (2×10^6 particles; one SPH particle has $10^3\ M_\odot$ and a softening length of ~ 50 pc), we demonstrate the growth and formation of a massive BH during hierarchical formation of a small spiral galaxy (with a total mass of $10^{10}\ M_\odot$). We found that the average rate of the mass accretion due to the radiation drag is $\approx 10^{-5}\ M_\odot\ {\rm yr^{-1}}$. Finally, a small spiral galaxy can have an IMBH with 10^4–$10^5\ M_\odot$ at $z \sim 4$.

Our model suggests that the growth of the massive BHs correlates not only with that of the galactic bulges, but also with that of the dark matter halos in the hierarchical formation of spiral galaxies. The massive BHs coevolve with the dark matter halo from $z \sim 15$ to 2. This means that the change in the dark matter potential closely correlates with the rate of the mass accretion onto a seed BH with the help of the radiation drag. The final mass ratio of the BH-to-dark matter halo is $\approx 10^{-6}$, and the final BH-to-bulge mass ratio is about 5×10^{-5} in a small spiral galaxy, which is much smaller than the observed value ($\approx 10^{-3}$) in the large galaxies due to the opacity effect, although the stellar feedback would affect on the result. Moreover, the time lag between the BH growth and the growth of the bulge (halo) would cause the scatter of the observed scaling relation.

In terms of the relationship between the AGN activity and the properties of host galaxies, we found that even a small spiral galaxy could show the same level of the typical low-luminosity AGNs with $L_{\rm AGN}/L_{\rm bulge} \approx 0.1$ at $z \approx 4$. Our model shows that the X-ray luminosity of the AGN is positively correlated with the CO luminosity (the gaseous mass) of the bulge very well. Furthermore, our result predicts that the BH-growing objects deviate from this scaling relation. By comparing our results with the properties of the LBGs, we predict that the LBGs could harbor massive BHs with 10^6–$10^7\ M_\odot$.

REFERENCES

Abadi, M. G., Navarro, J. F., Steinmetz, M., & Eke, V. R. 2003, ApJ, 591, 499
Adams, F., Graff, D. S., & Richstone, D. O. 2001, ApJ, 551, L31
Aller, M. C., & Richstone, D. 2002, AJ, 124, 3035
Baes, M., Buyle, P., Hau, G. K. T., & Dejonghe, H. 2003, MNRAS, 341, L44
Barnes, J., & Efstathiou, G. 1987, ApJ, 319, 575
Barth, A. J., Greene, J. E., & Ho, L. C. 2005, ApJ, 619, L151
Barth, A. J., Ho, L. C., Rutledge, R. E., & Sargent, W. L. W. 2004, ApJ, 607, 90
Bate, M. R., & Burkert, A. 1997, MNRAS, 288, 1060
Bertschinger, E. 2001, ApJS, 137, 1
Brandt, W. N., Hornschemeier, A. E., Schneider, D. P., Alexander, D. M., Bauer, F. E., Garmire, G. P., & Vignali, C. 2001, ApJ, 558, L5
Bukert, A., & Silk, J. 2001, ApJ, 554, L151

de Breuck, C., et al. 2003, A&A, 401, 911
Dietrich, M., & Wilhelm-Erkens, U. 2000, A&A, 354, 17
Di Matteo, T., Croft, R. A. C., Springel, V., & Hernquist, L. 2003, ApJ, 593, 56
Ferrarese, L. 2002, ApJ, 578, 90
Friaca, A. C. S., & Terlevich, R. J. 1999, MNRAS, 305, 90
Fukue, J., Umemura, M., & Mineshige, S. 1997, PASJ, 49, 673
Gordon, K., Calzetti, D., & Witt, A. N. 1997, ApJ, 487, 625
Granato, G. L., De Zotti, G., Silva, L., Bressan, A., & Danese, L. 2004, ApJ, 600, 580
Greene, J. E., & Ho, L. C. 2004, ApJ, 610, 722
Haehnelt, M. G. 2004, in Coevolution of Black Holes and Galaxies, ed. L. C. Ho (Cambridge: Cambridge Univ. Press), 406
Heaveans, A., & Peacock, J. 1988, MNRAS, 232, 339

Heckman, T. M., Blitz, L., Wilson, A. S., Armus, L., & Miley, G. K. 1989, ApJ, 342, 735

Heger, A., Fryer, C. L., Woosley, S. E., Langer, N., & Hartmann, D. H. 2003, ApJ, 591, 288

Hosokawa, T. 2004, ApJ, 606, 139

Imanishi, M., & Wada, K. 2004, ApJ, 617, 214

Jahnke, K., et al. 2004, ApJ, 614, 568

Katz, N. 1992, ApJ, 391, 502

Kauffmann, G., et al. 2003, MNRAS, 346, 1055

Kawakatu, N., & Umemura, M. 2002, MNRAS, 329, 572

———. 2004, ApJ, 601, L21

Kawakatu, N., Umemura, M., & Mori, M. 2003, ApJ, 583, 85

Kormendy, J., & Richstone, D. 1995, ARA&A, 33, 581

Magorrian, J., et al. 1998, AJ, 115, 2285

Maiolino, R., Juarez, Y., Mujica, R., Nagar, N. M., & Oliva, E. 2003, ApJ, 596, L155

Marconi, A., & Hunt, L. K. 2003, ApJ, 589, L21

Matteucci, F., & Pipino, A. 2002, ApJ, 569, L69

McLure, R. J., & Dunlop, J. S. 2002, MNRAS, 331, 795

Merritt, D., & Ferrarese, L. 2001, ApJ, 547, 140

Nandra, K., Mushotzky, R. F., Arnaud, K., Steidel, C. C., Adelberger, K. L., Gardner, J. P., Teplitz, H. I., & Windhorst, R. A. 2002, ApJ, 576, 625

Norman, C., & Scoville, N. 1988, ApJ, 332, 124

Ohsuga, K., & Umemura, M. 1999, ApJ, 521, L13

Ohta, K., Yamada, T., Nakanishi, K., Kohno, K., Akiyama, M., & Kawabe, R. 1996, Nature, 382, 426

Ostriker, J. P. 2000, Phys. Rev. Lett., 84, 5258

Saitoh, R. T., & Wada, K. 2004, ApJ, 615, L93

Salucci, P., Szuszkiewicz, E., Monaco, P., & Danese, L. 1999, MNRAS, 307, 637

———. 2000, MNRAS, 317, 488

Sanders, D. B., Soifer, B. T., Elias, J. H., Madore, B. F., Matthews, K., Neugebauer, G., & Scoville, N. Z. 1988, ApJ, 325, 74

Sato, J., Umemura, M., Sawada, K., & Matsuyama, S. 2004, MNRAS, 354, 176

Shankar, F., Salucci, P., Granato, G. L., De Zotti, G., & Danese, L. 2004, MNRAS, 354, 1020

Shapley, A. E., Steidel, C. C., Adelberger, K. L., Dickinson, M., Giavalisco, M., & Pettini, M. 2001, ApJ, 562, 95

Shibata, M. 2004, ApJ, 605, 350

Silk, J., & Rees, M. J. 1998, A&A, 331, L1

Spitzer, L., Jr. 1978, Physical Processes in the Interstellar Medium (New York: Wiley-Interscience)

Tsuribe, T., & Umemura, M. 1997, ApJ, 486, 48

Umemura, M. 2001, ApJ, 560, L29

Umemura, M., Fukue, J., & Mineshige, S. 1997, ApJ, 479, L97

Umemura, M., Loeb, A., & Turner, E. L. 1993, ApJ, 419, 459

Wada, K., Meurer, G., & Norman, C. A. 2002, ApJ, 577, 197

Wada, K., & Norman, C. 2001, ApJ, 547, 172

———. 2002, ApJ, 566, L21

Watabe, Y., & Umemura, M. 2005, ApJ, 618, 649

Yamada, T. 1994, ApJ, 423, L27

Yu, Q., & Tremaine, S. 2002, MNRAS, 335, 965

Zasov, A.V., Cherepashchuk, A. M., & Petrochenko, L. N. 2005, Astron. Rep., in press (astro-ph/0412560)